Journal of Saudi Chemical Society (2017) **21**, S240–S247

King Saud University

Journal of Saudi Chemical Society

www.ksu.edu.sa
www.sciencedirect.com

ORIGINAL ARTICLE

Fluorescent copper(II) complexes: The electron transfer mechanism, interaction with bovine serum albumin (BSA) and antibacterial activity

Madhumita Hazra [a,c], Tanushree Dolai [a], Akhil Pandey [b], Subrata Kumar Dey [c,*], Animesh Patra [a,*]

[a] *Department of Chemistry, Midnapore College, Midnapore 721101, India*
[b] *Department of Microbiology, Midnapore College, Midnapore 721101, India*
[c] *Department of Chemistry, Sidho-Kanho-Birsha University, Purulia, West Bengal, India*

Received 26 September 2013; revised 15 February 2014; accepted 16 February 2014
Available online 12 March 2014

KEYWORDS

Dinuclear copper complexes;
Optical properties;
BSA;
Antibacterial activity

Abstract Dinuclear copper(II) complexes with formula $[Cu_2(L)_2(N_3)_2]$ (**1**) and $[Cu_2(L)_2(NCS)_2]$ (**2**) **HL** = (1-[(3-methyl-pyridine-2-ylimino)-methyl]-naphthalen-2-ol) were synthesized by controlling the molar ratio of $Cu(OAC)_2{\cdot}6H_2O$, HL, sodium azide (**1**) and ammonium thiocyanate (**2**). The end on bridges appear exclusively in azide and thiocyanate to copper complexes. The electron transfer mechanism of copper(II) complexes is examined by cyclic voltammetry indicating copper(II) complexes are Cu(II)/Cu(I) couple. The interactions of copper(II) complexes towards bovine serum albumin (BSA) were examined with the help of absorption and fluorescence spectroscopic tools. We report a superficial solution-based route for the synthesis of micro crystals of copper complexes with BSA. The antibacterial activity of the Schiff base and its copper complexes were investigated by the agar disc diffusion method against some species of pathogenic bacteria (*Escherichia coli*, *Vibrio cholerae*, *Streptococcus pneumonia* and *Bacillus cereus*). It has been observed that the antibacterial activity of all complexes is higher than the ligand.

1. Introduction

The chiral molecule-based magnet design and synthesis is now of great interest because the chirality must be controlled in both the molecular structure and the entire crystal structure [12,11,5]. The basic strategy to design such materials is to organize paramagnetic centres into polynuclear aggregates or polymeric networks by use of bridging ligands that can efficiently propagate magnetic super exchange. Exchange interactions propagated by discrete poly atomic bridging

* Corresponding authors. Tel.: +91 9647309536.
E-mail addresses: skdjuchem@yahoo.com (S.K. Dey), animeshpatrarl@yahoo.com (A. Patra).

Peer review under responsibility of King Saud University.

ELSEVIER Production and hosting by Elsevier

http://dx.doi.org/10.1016/j.jscs.2014.02.009

moieties (NCO, NCS, N3, NCSe, etc.) between two paramagnetic centres have been the subject of several reviews [20,15] focusing on the ability of these pseudo halide ligands to coordinate with metals in a variety of ways. It is well-known that the azide anion is an efficient and versatile mediator for magnetic coupling, and pseudo halide-bridging ligands were more commonly employed in the design of poly nuclear transition-metal complexes with remarkable diversity in structure and magnetism [28,10]. The azide ion has the ability of binding two metal centres in a end-on (EO) or end-to-end (EE) fashion giving dinuclear or poly nuclear complexes [27,9]. Polynuclear metal azido complexes may also be formed due to the ability of the azide ligand to bind more than two metal centres [26]. This versatility of the azide ligand manifests itself in a variety of stereo chemistries, spectral and magnetic properties of the metal azido complexes.

The interaction between bio macromolecules and drugs has been drawing attention among researchers with great interest during last two decades [32,35]. Proteins are the most abundant macromolecules in cells and are crucial to maintaining normal cell functions. Among bio macromolecules, the serum albumins are the major soluble protein constituent of the circulatory system; they have many physiological functions [36]. Bovine serum albumin (BSA) has been one of the most extensively studied proteins, especially of its structural homology with human serum albumin [23]. BSA consists of three homologous domains (I, II, III) and each domain in turn is the product of two sub-domains [22]. BSA has two tryptophan residues, Trp–134 and Trp–212, which are embedded in the first sub-domain IB and sub-domain IIA, respectively [21]. Since the binding ability of a drug to serum albumin may have an importance in pharmacokinetics as well as the determination of the dosage form of the drug, the changes in fluorescence intensities of BSA-drug complex could give considerable information regarding the binding characteristics and the therapeutic effectiveness of drugs. Therefore, the binding of drugs to serum albumin in vitro, is considered as a model in protein chemistry to study the binding behaviour of proteins, research field in chemistry, life sciences and clinical medicine [30].

Herein we report an account of dinuclear copper(II) complexes with formula $[Cu_2(L)_2(N_3)_2]$ (**1**) and $[Cu_2(L)_2(NCS)_2]$ (**2**) HL = (1-[(3-methyl-pyridine-2-ylimino)-methyl]-naphthalen-2-ol). All the complexes have been characterized by spectroscopic methods. The electron transfer mechanism of copper(II) complexes is investigated by cyclic voltammetry. The BSA protein binding study of the copper(II) complexes has been performed spectroscopically. We report a superficial solution-based route for the synthesis of micro crystals of copper complexes with BSA. The complexes strongly bind to proteins, so we investigated the antibacterial activity of the Schiff base and its copper(II) complexes have also been studied by the agar disc diffusion method against some species of pathogenic bacteria (*Escherichia coli*, *Vibrio cholerae*, *Streptococcus pneumonia* and *Bacillus cereus*).

2. Experimental

2.1. Materials and physical measurements

All chemicals and reagents were obtained from commercial sources and used as received, unless otherwise stated. Solvents were distilled from an appropriate drying agent. The elemental (C, H, N) analysis was performed on a Perkin Elmer model 2400 elemental analyser. Copper analysis was carried out by a Varian atomic absorption spectrophotometer (AAS) model-AA55B, GTA using graphite furnace. Electronic absorption spectra were recorded on a SHIMADZU UV-1800 spectrophotometer. The fluorescence spectra of serum albumins were obtained in the Fluorimeter (Hitachi-2000). IR spectra (KBr discs, 4000–400 cm^{-1}) were recorded using a Perkin-Elmer FTIR model RX1 spectrometer. The room temperature magnetic susceptibility measurements were performed by using a vibrating sample magnetometer PAR 155 model. Molar conductances (M) were measured in a systronics conductivity metre 304 model using $\sim 10^{-3}$ mol L^{-1} solutions in appropriate organic solvents. Electron spray ionization (ESI) mass spectra were recorded on a Qtof Micro YA263 mass spectrometer. ^1H NMR spectral data were recorded in a suitable solvent using a Brucker 300, 400, 500 MHz FT-NMR spectrometer and ^{13}C NMR was recorded in a Bruker 400 MHz spectrometer using TMS as an internal standard in appropriate deuterated solvents. Electrochemical measurements were performed using computer-controlled CH-Instruments (Model No. CHI620D). All measurements were carried out under nitrogen environment at 298 K with reference to SCE electrode in dimethyl sulphoxide using $[n\text{-}Bu_4N]ClO_4$ as supporting electrolyte. The stock solutions of protein (1.00×10^{-4} mol L^{-1}) were prepared by dissolving the solid BSA in 0.05 M phosphate buffer at pH 7.4 and stored at 0–4 °C and then diluted to 1.20×10^{-6} mol L^{-1} using phosphate buffer (pH 7.4, 0.05 M) when used. The concentrations of BSA were determined from optical density measurements, using the values of molar absorptivity of $\varepsilon 280$ = 44,720 and 35,700 M^{-1} cm^{-1} for BSA [25,19]. Stock solutions of complexes **1** and **2** were prepared in DMF because of their lower solubility in water. The concentration of the copper(II) complexes (**1** and **2**) varied from 0–3.5×10^{-6} M. Powdered XRD was recorded in a 'Rigaku Miniflex-II' X-ray diffractometer using Cu-Kα radiation (λ = 0.154056 nm). Scans were collected on dry samples in the range of 10–80°. Optical microscopy images were taken using a NIKON ECLIPSE LV100POL upright microscope equipped with a 12 V–50 W halogen lamp. The samples for optical microscopic study were prepared by placing a drop of colloidal solution onto a clean glass slide.

2.2. Preparation of the ligand (HL)

The ligand **HL** was synthesized by adding 6.0 mmol of 2-hydroxy-naphthaldehyde and 6.0 mmol of 3-methyl-2-aminopyridine in 10 mL of ethanol in a round bottom flask with continuous stirring. The solution was stirred for 3 h and then refluxed up to 2 h and kept overnight to get the precipitate of the orange solid ligand. The precipitate was filtered by using a vacuum pump and washed several times using ethanol to remove any unreacted materials, finally crude product was collected by recrystallization in ethanol and dried the solid product as much as possible. Finally the product was characterized by IR, ^1H NMR and ^{13}C NMR spectroscopy.

$C_{17}H_{14}N_2O$: Anal. Found (%): C, 77.86; H, 5.34; N, 10.68; Calc.: C, 77.12; H, 5.48; N, 10.24, m.p. 186 ± 1 °C; EI-MS: $[M+H]^+$, m/z, 262.16; IR (KBr, cm^{-1}): ν_{O-H}, 3448, $\nu_{C=N}$, 1472, $\nu_{CH=N}$, 1623; ^1H NMR (δ, ppm in $CDCl_3$ + CCl_4):

15.686 (d, $1H_a$); 9.976 (d, $1H_b$); 8.30 (d,$1H_c$); 6.89 (d,$1H_d$); 8.15-7.04 (m, 9H); 2.498 (s, $1H_e$); ^{13}C NMR: 149.08 (C-9), 146.31 (C-1), 139.45 (C-7), 129.32–119.31 (Ar–C), 17.00 (C-6); Yield: 90%.

2.3. Preparation of $[Cu_2(L)_2(N_3)_2]$ (1) and $[Cu_2(L)_2(NCS)_2]$ (2)

The copper(II) complexes (**1** and **2**) were prepared by copper(II) acetate and the organic ligand (**HL**) in an equimolar ratio (1:1) (Scheme 1). A methanolic solution of **HL** (1.0 mmol) was mixed with 1.0 mmol of copper(II) acetate with constant stirring and then mixture was refluxed for 4 h. Then 2 ml of an aqueous solution of sodium azide (0.130 g, 2 mmol) for complex **1** and ammonium thiocyanate (0.154 g, 2 mmol) for complex **2** was added and stirring continued for 30 min. The solid product was collected by filtration. The solid product was washed with cold methanol and water respectively. The pure and dried crystallized product was obtained from methanol.

Complex **1**: $C_{34}H_{26}N_{10}O_2Cu_2$: Yield 80–85%; Anal. Found (%): C, 55.66; H, 3.54; N, 19.09; Cu, 17.32; Calc.: C, 55.82; H, 3.56; N, 19.12; Cu, 17.30. EI-MS: $[M+H]^+$, *m/z*, 733.15; IR (cm^{-1}): $\nu_{CH=N}$, 1618; $\nu_{C=N}$, 1470. m.p. 230 ± 1 °C. Magnetic moment (μ, B.M.): 1.46 per Cu atom. Conductivity (Λo, $ohm^{-1}\,cm^2\,mol^{-1}$) in DMF: 154.

Complex **2**: $C_{34}H_{26}N_{10}O_2Cu_2$: Yield 75–80%; Anal. Found (%): C, 56.47; H, 3.39; N, 10.98; Cu, 16.60; Calc.: C, 56.45; H, 3.37; N, 11.12; Cu, 16.58. EI-MS: $[M+H]^+$, *m/z*, 765.14; IR (cm^{-1}): $\nu_{CH=N}$, 1620; $\nu_{C=N}$, 1468. m.p. 238 ± 1 °C. Magnetic moment (μ, B.M.): 1.48 per Cu atom. Conductivity (Λo, $ohm^{-1}\,cm^2\,mol^{-1}$) in DMF: 148.

2.4. Protein binding experiments

The quantitative analysis of the interaction between copper(II) complexes and bovine serum albumin was performed by fluorimetric titration. The aqueous solution of protein was titrated by addition of the appropriate concentration of copper(II) complexes' (**1** and **2**) solution (to give a final concentration of 3.5×10^{-6} mol L^{-1}). For every addition, the mixture solution was shaken and allowed to stand for 20 min and then the fluorescence intensities were measured with an excitation wavelength of 280 nm.

2.5. Antimicrobial screening

The antibacterial activities of the ligand (**HL**) and its copper(II) complexes have been studied by the agar disc diffusion method [25,19]. The antibacterial activities were done at 100 and 200 μg/mL concentrations of different compounds in DMF solvent by using three pathogenic gram negative bacteria (*E. coli*, *V. cholerae*, *S. pneumoniae*) and one gram positive pathogenic bacteria (*B. cereus*). The DMF solvent was used as a negative control. The solution of ligand and its copper(II) complexes were added to the agar plates and incubated at 37 °C for 24 h. The diameter of the inhibition zones was measured in millimetres.

3. Results and discussion

3.1. Synthesis and characterization

The organic ligand (**HL** = (1-[(3-methyl-pyridin-2-ylimino)-methyl]-naphthalen-2-ol) was synthesized by the condensation reaction of 3-methyl-2-amino pyridine (6 mmol) with 6.0 mmol of 2-hydroxy-1-naphthaldehyde in ethanol. The complexes were obtained in good yield from the reaction of the copper acetate with azide (**1**), thiocyanate (**2**) with an equimolar amount of respective organic moiety **HL** in the methanol medium. In these complexes the organic molecule **HL** acts as tridentate ligand through N2O donor centres. The complexes' conductivity measurement in DMF shows conductance values [29] of 154 and 148 (Λo, $ohm^{-1}\,cm^2\,mol^{-1}$) suggesting that complexes exist in solution as non-electrolytes [6,7]. These coloured complexes are monomeric, air-stable, non-hygroscopic, partly soluble in ethanol, methanol, and fully soluble in DMF, acetonitrile. At room temperature the magnetic moments (μ) of these complexes are 1.46 and 1.48 B.M. per Cu atom which indicates all complexes are distorted trigonal bipyramidal geometry.

3.2. Infrared, NMR, mass spectra and electronic spectral studies

Infrared spectral data of the Schiff base show several bands at 3448, 1472 and 1623 cm^{-1} due to the phenolic O–H group, pyridine C=N and imine CH=N stretching vibrations in the solid state. The ligand also showed a broad and a weak

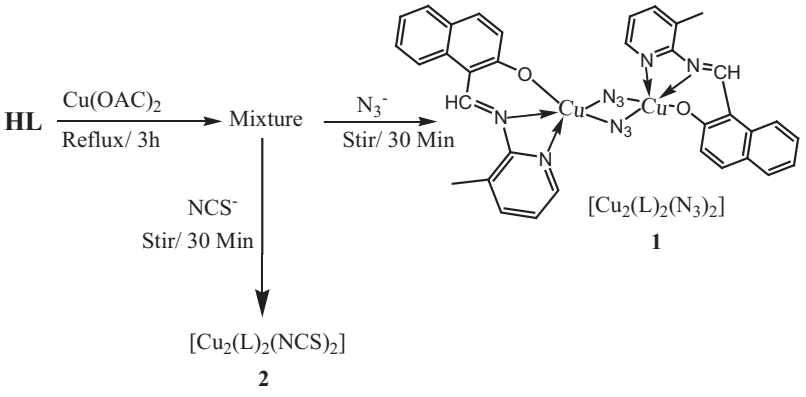

Scheme 1 Synthetic procedure of copper(II) complexes, for azide (**1**) and thiocyanate (**2**).

Table 1 UV–Vis spectral and electrochemical data of copper(II) complex **1** and **2**.

Compound	UV–Vis data λ, nm (ε, $dm^3\ mol^{-1}\ cm^{-1}$)[a]	Electrochemical data[a]		
		E_{pc} (V)	E_{pa} (V)	$E_{1/2}$ (V)
1	266(10,624), 320(8,125), 364(3,121), 662(230)	−0.984	−0.672	−0.828
2	258(9.710),325(6,498), 361(2,108), 668(169)	−0.958	−0.648	−0.803

[a] In DMF; Electrochemical data recorded in mV, at 298 K and scan rate 100 mVs^{-1}; $E_{1/2} = (E_{pc} + E_{pa})/2$.

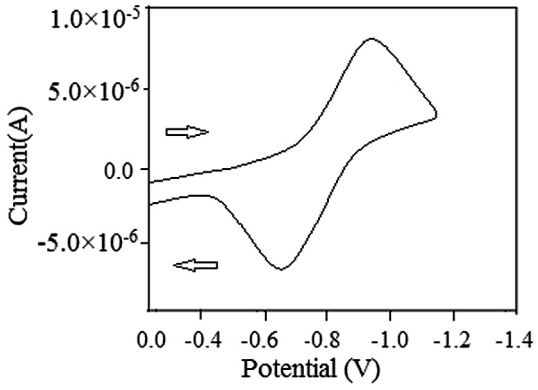

Figure 1 Cyclic voltammograms of complex 1.

band in the region 2850–2730 cm^{-1}, which confirms the intra molecular hydrogen-bonded OH group. The bands are shifted to lower frequency on complexation with copper(II) ions. New vibrations at 406–414 and 510–514 cm^{-1} which are not present in the free Schiff base are attributed to the existence of Cu—O and Cu—N bonds. IR spectrum of the complexes showed a strong absorption band at 2035 cm^{-1} [37] indicating azido ligand and a band at 2024 cm^{-1} indicating thiocyanate ligands. All the IR data suggest that the metal ions are bonded to the Schiff base through the phenolic oxygen, pyridine nitrogen and the imino-nitrogen, azide (**1**) and thiocyanide (**2**).

The ^1H NMR spectra (Fig. S1) of the ligand have been recorded in $CDCl_3$ at room temperature using CCl_4 as an internal standard. The ligand exhibits hydroxyl proton (H_a) that appeared at δ 15.68 ppm, H_b appeared at δ 9.97 ppm, H_c appeared at δ 8.30 ppm, H_d appeared at δ 6.89 ppm, methyl proton (H_e) appeared at δ 2.49 ppm, aromatic and heteroaromatic proton signals at δ 7.04–8.15 ppm. The chemical shift of hydroxyl proton is very high (15.68 ppm) indicating intra molecular hydrogen bond. ^{13}C NMR spectra (Fig. S2) showed similar diagnostic features for the free ligand. Hydroxyl carbon (C-9) was found at 149.08 ppm, pyridine carbon (C-1) at 146.31 ppm, imine carbon (C-7) at 139.45 ppm, and the methyl carbon (C-6) signal was found at 17.0 ppm and aromatic carbons at 119.3–129.3 ppm. NMR spectra of the free ligand support the conclusions derived from the IR spectra. The mass spectrum of the copper(II) complexes also supports its projected formulation. The mass spectra of complexes were recorded and it indicates the molecular ion peak m/z at 262.16, consistent with the molecular weight of the ligand, whereas its copper complex (**1**) shows the molecular ion peak at m/z 733.15, 522, 408, 366, 324 which confirms the stoichiometry of the copper complexes to be $[Cu_2L_2(N_3)_2]$. Similarly copper thiocyanate (**2**) complex shows respective mass spectra. The spectra of the complex (**1**) are shown in Fig. S3.

The electronic spectra of all complexes were recorded in DMF at room temperature. The electronic spectral data of the Schiff base and their complexes are given in Table 1. All the spectra of complexes show lower bands than 400 nm that are due to intramolecular $\pi \rightarrow \pi^*$ and $n \rightarrow \pi^*$ transitions for the aromatic ring. An intense band at 258 nm is assigned to $\pi \rightarrow \pi^*$ intra-ligand transition [3] along with the less intense bands at 320 and 325 nm corresponding to the ligand to metal charge transfer transition. A broad band observed at 662 and 668 nm for complex **1** and **2** is well in agreement with the d–d transition for copper(II) in the distorted TBP geometry [18].

3.3. Electrochemistry

The redox properties of the copper(II) complexes were examined by cyclic voltammetry using a Pt-disc working electrode and a Pt-wire auxiliary electrode in dry dimethylformamide using $[n\text{-}Bu_4N]ClO_4$ (0.1 M) as the supporting electrolyte. The cyclic voltammetric data are given in Table 1. The cyclic voltammograms exhibit quasi-reversible electron transfer process with a reduction peak at $E_{pc} = -0.984$ and −0.958 V with a corresponding oxidation peak at $E_{pa} = -0.672$ and −0.648 V for complexes of **1** and **2** at a scan rate interval 50–400 mV s^{-1} [17]. The most significant characteristic of the copper(II) complexes is the Cu(II)/Cu(I) couple given in Fig. 1. The ratio of cathodic to anodic peak height was less than one. However, the peak current increases with the increase of the square root of scan rates. From these data, it can be deduced that the redox couple is related to a quasi-reversible one-electron transfer process controlled by diffusion.

3.4. Powder diffraction studies

The single crystal of the complexes could not be prepared to get the XRD and hence the powder diffraction data were also used to investigate the molecular connectivity and crystalline nature of complexes. An X-ray powder diffraction pattern of copper complexes (**1** and **2**) has been given in Fig. 2. All the sharp peaks of the different scale particles mean that they all are crystalline in nature. The XRD of different scale particles are well coincident with each other and it means that different forms of complexes have the same structure. No peaks characteristic of impurities are detected in the XRD patterns.

3.5. Emission activity

The emission property of the ligand **HL** and its copper(II) complexes were recorded at room temperature (298 K) in 1×10^{-6} (M) DMF solution given in Fig. 3. Generally, fluorescence behaviour of a ligand quenched by complex formation is a familiar phenomenon, which is explained by the processes such as electronic energy transfer, magnetic perturbation,

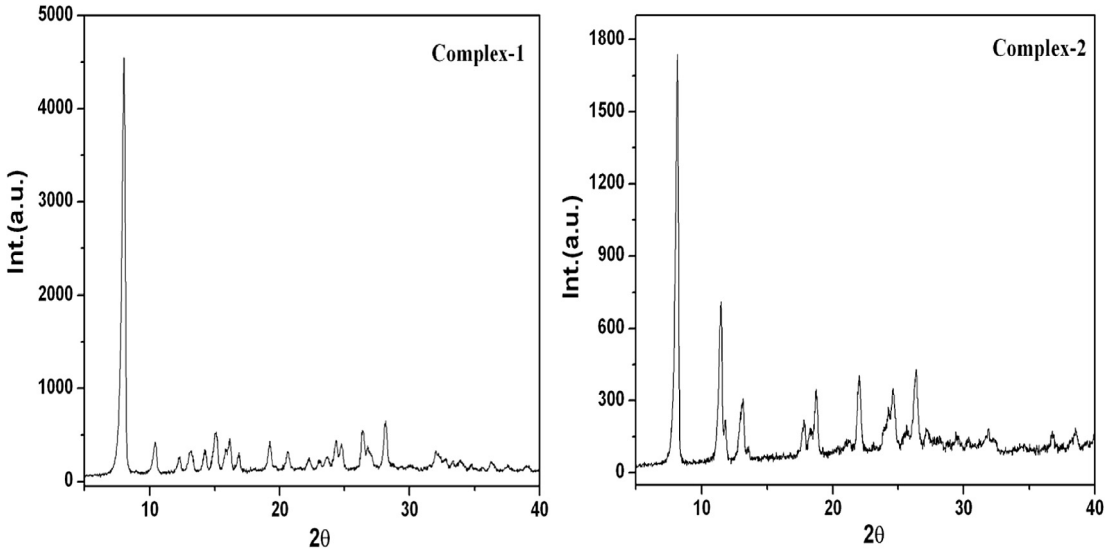

Figure 2 Powder XRD of complex **1** and **2**.

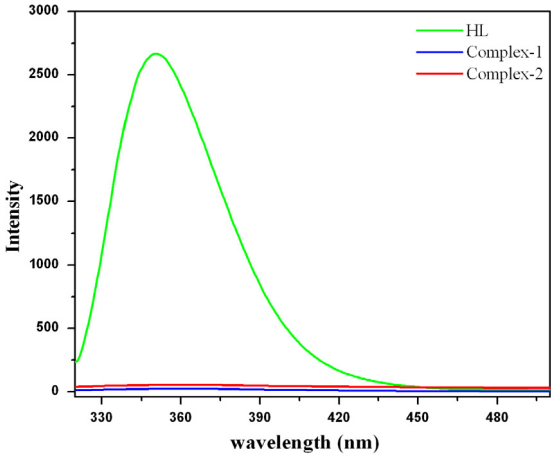

Figure 3 Fluorescence emission spectra of the free ligand (**HL**) and its copper(II) complexes.

redox activity, etc. [16]. These copper(II) complexes (**1** and **2**) make the energy transfer from the excited state of the ligand to the metal ions causing decreases of the fluorescence intensity. For this reason the fluorescence intensity of complex **1** and **2** is decreased.

3.6. BSA binding experiments

3.6.1. Absorption characteristics of BSA–Cu(II) complexes

The absorption spectra of BSA in the absence and presence of copper(II) complexes were studied at different concentrations in phosphate buffer, pH 7.4. It has been observed that absorption of BSA increases regularly upon increasing the concentration of the complexes (Fig. 4). The increasing absorption may be due to the adsorption of BSA on the surface of the complex. The apparent association constant (K_{app}) determined using the Benesi–Hildebrand equation [2]:

$$1/(A_{obs} - A_0) = 1/(A_c - A_0) + 1/K_{app}(A_c - A_0)[comp]$$

where, A_{obs} is the observed absorbance of the solution containing different concentrations of the complex at 280 nm. A_0 and A_c are the absorbance of BSA only and BSA with complex respectively. K_{app} represents the apparent association constant. The enhancement of absorbance at 280 nm was due to adsorption of the surface complex, based on the linear relationship between $1/(A_{obs} - A_0)$ and reciprocal concentration of the complex (Fig. S4) with a slope equal to $1/K_{app}(A_c - A_0)$ and an intercept equal to $1/(A_c - A_0)$. The value of the apparent association constant (K_{app}) determined from this plot is $4.26 \times 10^4\ M^{-1}$ ($R = 0.9945$) and $3.92 \times 10^4\ M^{-1}$ ($R = 0.9913$) for complexes **1** and **2** respectively. All the values suggested strong affinity of complex to protein and plots represent a good linear relationship.

3.6.2. Fluorescence quenching of BSA by the copper complexes

The interaction of copper(II) complexes with BSA were studied by the fluorescence emission spectrum of BSA with increasing the concentration of the copper complexes. The emission spectra of BSA in the presence of different concentrations of complexes were recorded in the wavelength range 300–500 nm by exciting the protein at 280 nm represented in Fig. 5. As seen, in both cases, with increasing the concentration of the copper complexes the fluorescence intensities of the proteins are regularly decreased [38]. The fluorescence quenching is described by the Stern–Volmer relation [33]

$$I_0/I = 1 + K_{sv}[Q]$$

where I_0 and I represent the fluorescence intensity in the absence and presence of quencher respectively. K_{sv} is a linear Stern–Volmer quenching constant and Q is the concentration of quencher. In case of fluorescence quenching of BSA a linear plot between I_0 and I against [complex] was obtained (Fig. S5) and from the slope we calculated the K_{sv} that is $3.60 \times 10^5\ M^{-1}$ ($R = 0.9789$) and $3.46 \times 10^5\ M^{-1}$ ($R = 0.9870$) for complex **1** and **2** respectively. The binding constant values suggest that complexes strongly bind to albumins. As it is known, linear Stern–Volmer plots represent a single quenching mechanism, either static or dynamic [8].

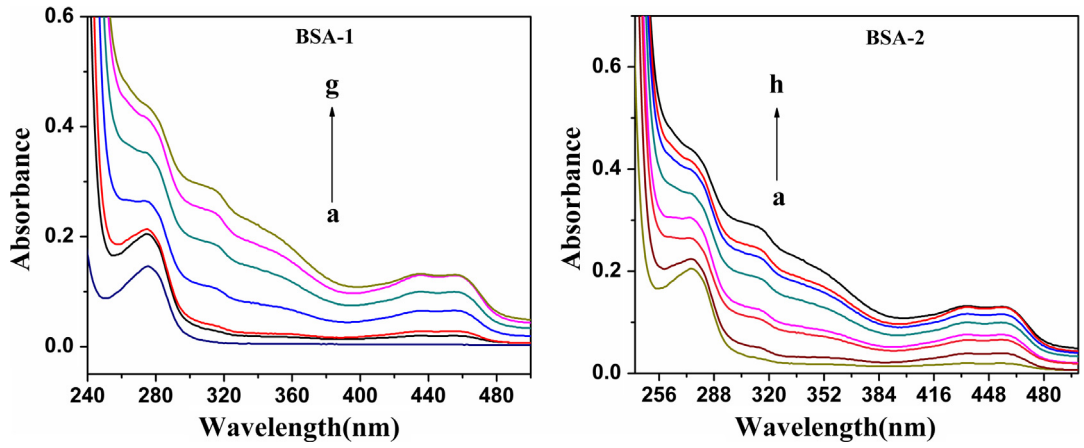

Figure 4 Electronic spectral titration of complex **1** (BSA-1) and **2** (BSA-2) with BSA in the presence of phosphate buffer, pH 7.4. The concentration of complex varied from (a) 0.0 to (g) 3.5×10^{-6} M L^{-1}. Arrow indicates an increase in the concentration of complex.

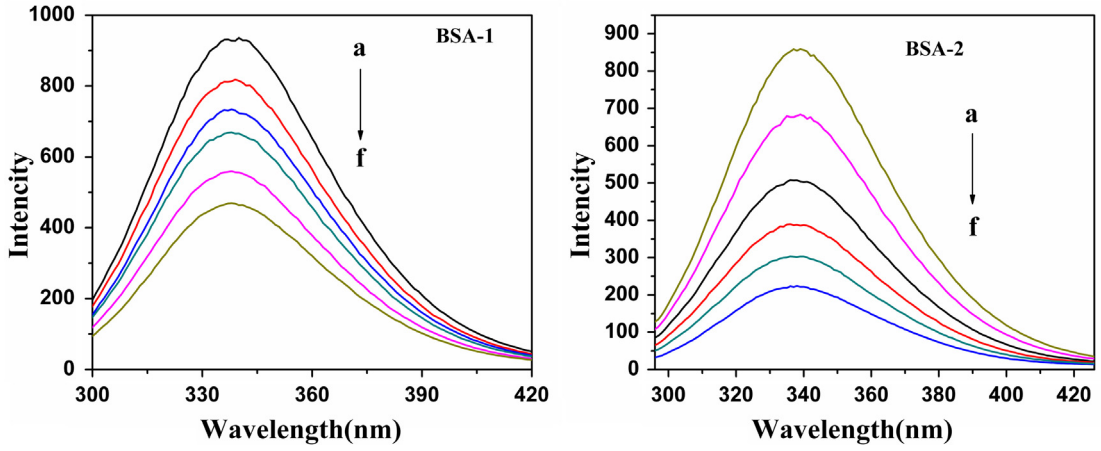

Figure 5 Change in fluorescence spectra of complex **1** (BSA-1) and **2** (BSA-2) with BSA, excited at 266 nm in the presence of phosphate buffer, pH 7.4. The concentration of complex varied from (a) 0.0 to (g) 3.5×10^{-6} M L^{-1}. Arrow indicates an increase in the concentration of complex.

3.6.3. Analysis of binding sites

Number of binding sites can be calculated from fluorescence titration data using the following equation [14]

$$\log[(I_0 - I)/I] = \log K_b + n\log[Q]$$

K_b and n are the binding constant and binding site of Cu(II) complexes. According to the experimental results, the linear fitting plots of $\log[(I_0 - I)/I]$ vs. $\log[Q]$ can be observed (Fig. S6). The corresponding K_b and n values were evaluated from the slopes and intercepts of the linear plots, respectively. The binding constant and number of binding sites (n) are given in Table S1. The binding constant (K_b) value indicates Cu(II) complexes strongly bind to BSA. Again, the value of n is nearly 1 for binding of both complexes to the protein used, which indicates the high affinity binding sites of albumins.

3.7. Fluorescence microscopy study for crystallization of Cu–BSA complexes

The optical and fluorescence micrograph in Fig. 6 showed formation of rod shaped copper complex with BSA. The obtained yellowish-green and bluish green micro rods were characterized by using fluorescence microscopy to investigate their optical waveguide properties. This suggests that the Cu complexes' (**1** and **2**) molecules have been incorporated into the BSA microparticles during the solution-based route process, and they are likely to be distributed randomly in the nano particles. It is supposed that during the formation of the doped microparticles, hydrophobic and π–π interactions induce the aggregation of BSA and Cu complexes' (**1** and **2**) molecules into micro particles. Fascinatingly, the uniform microrods exhibited yellowish-green emission with very bright luminescence spots at both tips and relatively weaker emission from the bodies of the rods, which is characteristic of an optical waveguide [4,34]. This observation suggested that the microrods absorbed the excitation light and propagated the fluorescence emission towards the tips, thereby exhibiting strong wave guiding behaviour. The remarkable optical waveguide properties could be related to the single-crystalline nature and the strong fluorescence emission behaviour of the BSA-Cu complex microrods.

3.8. Antibacterial activity

Antibacterial activity of the ligand and its copper(II) complexes are given in Table S2. The biological activity of the

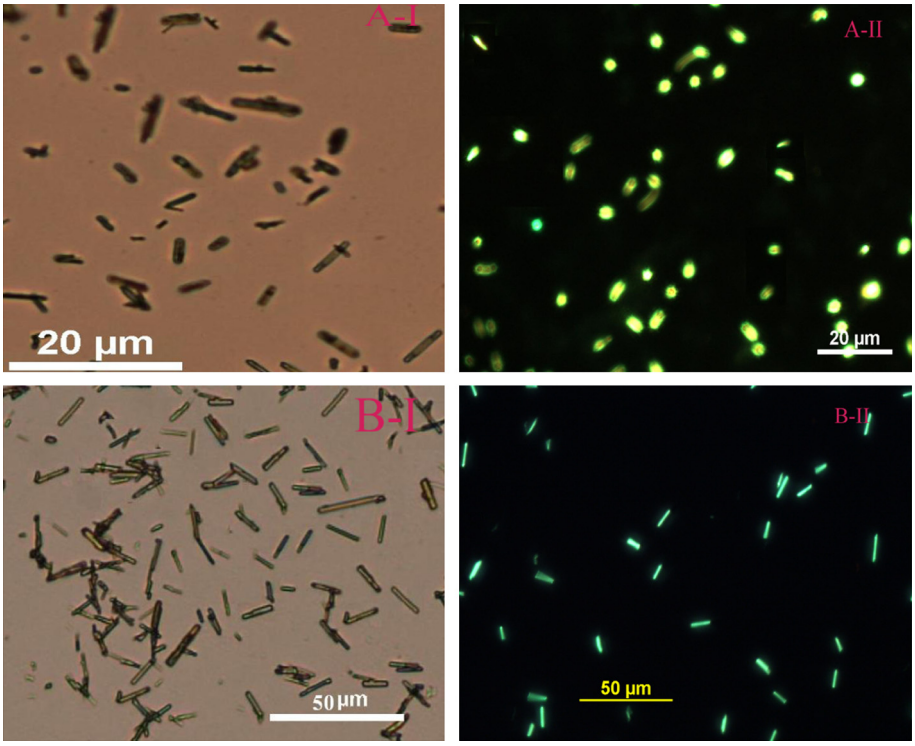

Figure 6 Optical and fluorescence micrographs of complex **1** (A-I and A-II) and complex **2** (B-I and B-II) with BSA microrods respectively. The fluorescence micrograph was obtained by the excitation of the sample with blue light between 450 and 490 nm.

ligand and complexes were compared with standard antibiotic Chloramphenicol in presence of gram positive and gram negative bacteria.From the studies it is inferred that, all complexes have higher activity than ligand but lower than antibiotic [31,13]. The metal chelates are higher activity than freeligand. It can be explained by overtone concept and the Tweedy chelation theory [24]. The variation in the activity of copper(II) complexes against some different organisms depends either on the impermeability of the cells of the microbes or difference in ribosome of microbial cells and also activity increases with an increase in the concentration of complexes [1]. It is observed that, in a complex, the metal positive charge is partially shared with the ligand; which increases the delocalization of pi-electrons over the whole chelate ring, favours the lipophilic character of the metal complexes. This increased lipophilicity enhances the penetration of complexes into the lipid layer of the bacterial cell membranes and blocks the metal binding sites in enzymes of microorganisms. These complexes also disturb the respiration process of the cell and thus block the synthesis of proteins, which restricts further growth of the microorganisms. Due to higher lipophilicity, complex **1** and **2** exhibit higher antibacterial activity than free ligand.

4. Conclusion

Synthesis and characterization of two dinuclear copper(II) complexes of N2O donor set have been performed. All complexes are penta-coordinated formulated as formula $[Cu_2(L)_2(N_3)_2]$ (**1**) and $[Cu_2(L)_2(NCS)_2]$ (**2**). The electrochemical study of copper(II) complexes demonstrated a quasi-reversible one-electron transfer process. BSA binding of copper(II) complexes are investigated by absorption and fluorescence spectroscopic tools and quenching mechanism may be static or dynamic. All copper(II) complexes bind to BSA giving microcrystals. The ligand and its copper(II) complexes displayed promising antibacterial activity compared to known antibiotic drug.

Acknowledgement

We are thankful to Prof. Pabitra Chattopadhyay, Dept. of Chemistry, Burdwan University, Burdwan, for allowing us to do the electrochemical measurement.

Appendix A. Supplementary data

Supplementary data associated with this article can be found, in the online version, at http://dx.doi.org/10.1016/j.jscs.2014.02.009.

References

[1] G.B. Bagihalli, P.G. Avaji, S.A. Patil, P.S. Badami, Synthesis, spectral characterization, in vitro antibacterial, antifungal and cytotoxic activities of Co(II), Ni(II) and Cu(II) complexes with 1,2,4-triazole Schiff bases, Eur. J. Med. Chem. 43 (2008) 2639–2649.

[2] H.A. Benesi, J.H. Hildebrand, A spectrophotometric investigation of the interaction of iodine with aromatic hydrocarbons, J. Am. Chem. Soc. 71 (1949) 2703–2707.

[3] B.H. Chen, H.H. Yao, W.T. Huang, P. Chattopadhyay, J.M. Lo, T.H. Lu, Syntheses and molecular structures of three Cu(II) complexes with tetradentate imine-phenols, Solid State Sci. 1 (1999) 119–131.

[4] W. Chen, Q. Peng, Y. Li, Luminescent Bis-(8-hydroxyquinoline) cadmium complex nanorods cryst, Growth Des. 8 (2008) 564–567.
[5] E. Coronado, F. Palacio, J. Veciana, Molecule-based magnetic materials, Angew. Chem. Int. Ed. 42 (2003) 2570–2572.
[6] S. Dey, S. Sarkar, H. Paul, E. Zangrando, P. Chattopadhyay, Copper(II) complex with tridentate N donor ligand: synthesis, crystal structure, reactivity and DNA binding study, Polyhedron 29 (2010) 1583–1587.
[7] S. Dey, T. Mukherjee, S. Sarkar, H.S. Evans, P. Chattopadhyay, 5-Nitro-1,10-phenanthroline bis(N, N-dimethylformamide-K′O)-bis(perchlorato) copper(II): synthesis, structural characterization, and DNA-binding study, Trans. Met. Chem. 36 (2011) 631–636.
[8] M.R. Eftink, C.A. Ghiron, Fluorescence quenching of indole and model micelle systems, J. Phys. Chem. 80 (1976) 486–493.
[9] E. Escuer, R. Vicente, J. Ribas, Magnetic transition in ferromagnetically coupled dimer of Ni(II) with di-μ-azido bridge, J. Magn. Magn. Mater. 110 (1992) 181–184.
[10] E.Q. Gao, Y.F. Yue, S.Q. Bai, Z. He, C.H. Yan, From achiral ligands to chiral coordination polymers: spontaneous resolution, weak ferromagnetism, and topological ferrimagnetism, J. Am. Chem. Soc. 126 (2004) 1419–1429.
[11] H. Imai, K. Inoue, K. Kikuchi, Y. Yoshida, M. Ito, T. Sunahara, S. Onaka, Three-dimensional chiral molecule-based ferrimagnet with triple-helical-strand structure, Angew. Chem. Int. Ed. 43 (2004) 5618–5621.
[12] K. Inoue, K. Kikuchi, M. Ohba, H. Ookawa, Structure and magnetic properties of a chiral two-dimensional ferrimagnet with TC of 38 K, Angew. Chem. Int. Ed. 42 (2003) 4810–4813.
[13] J. Joseph, K. Nagashri, G. Ayisha Bibin Rani, Synthesis, characterization and antimicrobial activities of copper complexes derived from 4-aminoantipyrine derivatives, J. Saudi Chem. Soc. 17 (2013) 285–294.
[14] A. Kathiravan, R. Renganathan, Photoinduced interactions between colloidal TiO_2 nanoparticles and calf thymus-DNA, Polyhedron 28 (2009) 1374–1378.
[15] O. Kahn, Y. Pei, Y. Journaux, in: Q.W. Bruce, D. O'Hare (Eds.), Inorganic Materials 2nd ed., Wiley, Chichester, UK, 1997.
[16] S. Konar, A. Jana, K. Das, S. Ray, S. Chatterjee, J.A. Golen, A.L. Rheingold, S.K. Kar, Synthesis, crystal structure, spectroscopic and photoluminescence studies of manganese(II), cobalt(II), cadmium(II), zinc(II) and copper(II) complexes with a pyrazole derived Schiff base ligand, Polyhedron 30 (2011) 2801–2808.
[17] A.D. Kulkarni, S.A. Patil, P.S. Badami, Electrochemical properties of some transition metal complexes: synthesis, characterization and in-vitro antimicrobial studies of Co(II), Ni(II), Cu(II), Mn(II) and Fe(III) complexes, Int. J. Electrochem. Sci. 4 (2009) 717–729.
[18] Y. Nakao, M. Onoda, T. Sakurai, A. Nakahara, I. Kinoshita, S. Ooi, Copper(II) complexes with tripodal imidazole-containing ligands. Structure–electrochemistry relationship, Inorg. Chim. Acta 151 (1988) 55–59.
[19] N.S. Ng, P. Leverett, D.E. Hibbs, Q. Yang, J.C. Bulanadi, M.J. Wu, J.R. Aldrich-Wright, The antimicrobial properties of some copper(II) and platinum(II) 1,10-phenanthroline complexes, Dalton Trans. 42 (2013) 3196–3209.
[20] A.H. Norbury, A.I.P. Sinha, The co-ordination of ambidentate ligands, Q. Rev. Chem. Soc. 24 (1970) 69–94.
[21] R.E. Olson, D.D. Christ, Chapter 33. Plasma protein binding of drugs, Ann. Rep. Med. Chem. 31 (1996) 327–336.
[22] A. Papadopoulou, R.J. Green, R.A. Frazier, Interaction of flavonoids with bovine serum albumin: a fluorescence quenching study, J. Agric. Food Chem. 53 (2005) 158–163.
[23] T.J. Peters, Serum albumin, Adv. Protein Chem. 37 (1985) 161–245.
[24] N. Raman, A. Kulandaisamy, A. Shunmugasundaram, K. Jeyasubramanian, Synthesis, spectral, redox and antimicrobial activities of Schiff base complexes derived from 1-phenyl-2,3-dimethyl-4-aminopyrazol-5-one and acetoacetanilide, Trans. Met. Chem. 26 (2001) 131–135.
[25] N. Raman, S. Sobha, L. Mitu, Design, synthesis, DNA binding ability, chemical nuclease activity and antimicrobial evaluation of Cu(II), Co(II), Ni(II) and Zn(II) metal complexes containing tridentate Schiff base, J. Saudi Chem. Soc. 17 (2013) 151–159.
[26] J. Reedjik, Electronic spectra and electron spin resonance of tetragonal copper(II) N-alkyl imidazole compounds, Trans. Met. Chem. 6 (1981) 195–197.
[27] J. Ribas, M. Monfort, B.K. Ghosh, R. Cortes, X. Salonas, M. Font-Bordia, Two new antiferromagnetic nickel(II) complexes bridged by azido ligands in the Cis position. Effect of the Counteranion on the crystal structure and magnetic properties, Inorg. Chem. 35 (1996) 864–868.
[28] J. Ribas, A. Escuer, M. Monfort, R. Vicente, R. Cortes, L. Lezama, T. Rojo, Polynuclear NiII and MnII azido bridging complexes. Structural trends and magnetic behaviour, Coord. Chem. Rev. 193–195 (1999) 1027–1068.
[29] S. Sarkar, H. Paul, M.G.B. Drew, E. Zangrando, P. Chattopadhyay, Synthesis, crystal structure and reactivity of copper(II) complexes of tetradentate N2S2 donor ligands, J. Mol. Struct. 933 (2009) 126–131.
[30] A. Schepartez, B. Cuenoud, Site-specific cleavage of the protein calmodulin using a trifluoperazine-based affinity reagent, J. Am. Chem. Soc. 112 (1990) 3247–3249.
[31] R.A. Sheikh, S. Shreaz, G.S. Sharma, L.A. Khan, A.A. Hashmi, Synthesis, characterization and antimicrobial screening of a novel organylborate ligand, potassium hydro(phthalyl)(salicylyl)borate and its Co(II), Ni(II), and Cu(II) complexes, J. Saudi Chem. Soc. 16 (2012) 353–361.
[32] S. Soares, N. Mateus, V. De Freitas, Interaction of different polyphenols with bovine serum albumin (BSA) and human salivary α-amylase (HSA) by fluorescence quenching, J. Agri. Food Chem. 55 (2007) 6726–6735.
[33] O. Stern, M. Volmer, On the quenching-time of fluorescence, Z. Phys. 20 (1919) 183–188.
[34] K. Takazawa, Waveguiding properties of fiber-shaped aggregates self-assembled from thiacyanine dye molecules, J. Phys. Chem. C 111 (2007) 8671–8676.
[35] Y.Q. Wang, H.M. Zhang, G.C. Zhang, W.H. Tao, Z.H. Fei, Z.T. Liu, Spectroscopic studies on the interaction between silicotungstic acid and bovine serum albumin, J. Pharmaceut. Biomed. Anal. 43 (2007) 1869–1875.
[36] X.L. Wei, J.B. Xiao, Y.F. Wang, Y.L. Bai, Which model based on fluorescence quenching is suitable to study the interaction between trans-resveratrol and BSA?, Spectrochim Acta Part A: Mol. Biomol. Spectrosc. 75 (2010) 299–304.
[37] X.M. Zhang, Y.Q. Wang, Y. Song, E.Q. Gao, Synthesis, structures, and magnetism of copper(II) and manganese(II) coordination polymers with azide and pyridylbenzoates, Inorg. Chem. 50 (2011) 7284–7294.
[38] X.P. Zhang, Y.H. Hou, L. Wang, Y.Z. Zhang, Y. Liu, Exploring the mechanism of interaction between sulindac and human serum albumin: spectroscopic and molecular modeling methods, J. Lumin. 138 (2013) 8–14.